JOURNAL OF VIROLOGY, July 1994, p. 4227–4240
0022-538X/94/$04.00+0

Vol. 68, No. 7

Simian Virus 40 Large T Antigen Host Range Domain Functions in Virion Assembly

SUSAN L. SPENCE AND JAMES M. PIPAS*

Department of Biological Sciences, University of Pittsburgh, Pittsburgh, Pennsylvania 15260

Received 11 November 1993/Accepted 4 April 1994

The simian virus 40 (SV40) T antigen host range mutants *dl*1066 and *dl*1140 display a postreplicative block to plaque formation which suggests a novel role for T antigen late in the viral life cycle. The host range mutants *dl*1066 and *dl*1140 are able to grow in and plaque on BSC but not on CV1 monkey kidney cells, a normally permissive host. Previous work showed that in CV1 cells infected with *dl*1066 and *dl*1140, levels of viral DNA replication and of late capsid protein accumulation were only slightly reduced and the failure to accumulate agnoprotein was not likely to be the major factor responsible for the mutants' growth defect. Here we show that the host range mutants are defective in the assembly of viral particles. SV40 assembly proceeds as the progressive conversion of 75S viral chromatin complexes to 200S-240S assembled virions. When virus-infected cell extracts are separated on 5 to 40% sucrose gradients, wild-type extracts show the greatest accumulation of viral late protein in the 200S-240S fractions corresponding to the assembled virus peak and lesser amounts in the 75S-150S fractions corresponding to immature assembly intermediates. The host range mutants *dl*1066 and *dl*1140 grown in nonpermissive CV1 cells, however, failed to assemble any appreciable amounts of mature 200S-240S virions and accumulate 75S intermediates, whereas in permissive BSC cells, levels of assembly were more slightly reduced than those of the wild type. Analysis of the protein composition of gradient fractions suggests that SV40 assembly proceeds by a mechanism similar to that proposed for polyomavirus and suggests that the host range blockage may result from a failure of such mutants to add VP1 to 75S assembly intermediates.

As the multifunctional master regulatory protein of simian virus 40 (SV40), large T antigen encodes a variety of activities which enable the virus to grow efficiently in monkey cells and to transform rodent cells. During productive infection, large T antigen is necessary for the initiation and maintenance of viral DNA replication, for autoregulation of early gene expression, and for stimulation of late gene expression. T antigen also stimulates cell DNA synthesis and the transcription of some host genes. Its activities include a sequence-specific DNA binding activity which enables T antigen to bind to the viral replication origin, ATPase and DNA helicase activities, one or more transcriptional transactivation activities, and the ability to bind to a number of cellular proteins, most notably the tumor-suppressor protein p53 and the retinoblastoma susceptibility gene product, Rb (20, 22).

All T antigen functions required for viral DNA replication, transcriptional control, and neoplastic transformation are localized to the N terminus and middle portion of the protein (12, 17, 60, 67). The role of the C terminus of T antigen (amino acids 660 to 708) in lytic growth of SV40 has been less well understood. In fact, the C terminus can be deleted with only minimal effects on virus yield and plaque size upon growth of the virus in BSC cells at 37°C. However, the last 26 amino acids of T antigen, which retain host range activity (65), are highly conserved among the primate papovaviruses, and two lines of investigation have uncovered conditions under which there is an absolute requirement for the C terminus of SV40 T antigen for viral growth in monkey cells.

Early investigators first described the C terminus as containing an adenovirus-helper function, having found that this part of T antigen is sufficient to enable the growth of human adenoviruses in BSC and CV1 monkey cells. Human adenoviruses grow efficiently in human cells but grow 1,000-fold less efficiently in African green monkey kidney cell lines. Late gene transcription at the major late promoter is 2- to 10-fold reduced (39), probably by premature termination or attenuation (35). In addition, synthesis of the fiber capsid protein is further reduced by approximately 100-fold, purportedly by inappropriate splicing, reduced translation, and other unidentified factors (1, 2, 40, 58). The block to productive infection can be relieved either by a helper function supplied by the carboxy-terminal fragment of SV40 large tumor antigen (15, 30, 37, 53) or by a mutation localized to the N-terminal domain of the multifunctional adenovirus 72-kDa DNA-binding protein, whose carboxy-terminal domain, reminiscent of T antigen, is responsible for DNA binding, replication, transcriptional autoregulation, enhanced transformation, and assembly of adenovirus (10, 41). In the presence of either of these elements, attenuation of late transcription is reduced and proper processing of the fiber message is restored.

More recently, the C terminus of T antigen has been described as containing a host range activity. Whereas SV40 strains carrying deletions of the C terminus of T antigen are able to grow in BSC African green monkey kidney cells, they are unable to grow in CV1 monkey kidney cells (50, 64, 65). Moreover, growth in permissive cells is temperature sensitive: the mutant viruses grow in BSC cells at 37°C but do not grow in this line at 32°C (16, 50). Compared with wild-type virus, mutant stocks give 10-fold-lower yields on BSC cells and 10,000-fold-lower yields on CV1 cells (50). Mutant viruses replicate DNA at nearly wild-type levels under nonpermissive conditions, suggesting a postreplicative block to lytic growth similar to the adenovirus helper function block (50, 64). The properties of all mutants studied to date suggest that the host

* Corresponding author. Mailing address: Department of Biological Sciences, University of Pittsburgh, Pittsburgh, PA 15260. Phone: (412) 624-4691. Fax: (412) 624-4759.

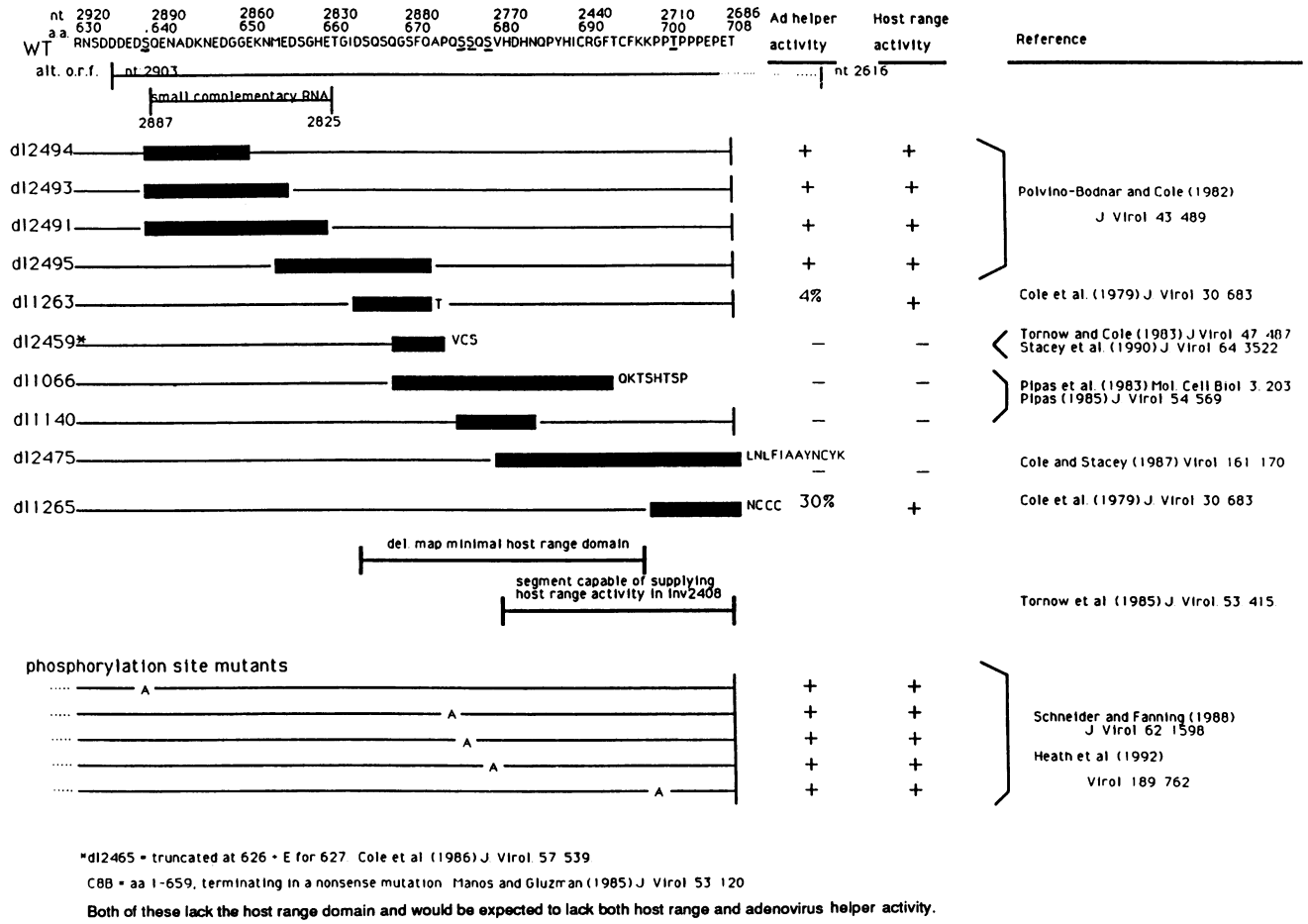

FIG. 1. Summary of host range mutants. At the top, the sequence of the carboxy-terminal region of T antigen with corresponding amino acid and nucleotide positions is shown. The positions of deletion mutants and amino acid substitution mutants within the carboxy-terminal domain are indicated, and the positions of phosphorylated amino acids are shown. Sequences important for adenovirus helper function and host range activities are indicated.

range activity and the adenovirus helper activity are identical (Fig. 1).

To date, the stage at which the host range defect blocks lytic infection has remained elusive. In previous work we demonstrated that in nonpermissive cells infected with SV40 T antigen host range mutants *dl*1066 and *dl*1140, accumulation of the viral capsid proteins VP1, VP2, and VP3 was only slightly reduced (38). The host range mutants did fail to make detectable levels of the late leader-encoded agnoprotein (38). However, this appeared not to be the major factor responsible for their growth defect. Agnoprotein mutants exhibit a much less severe phenotype, and the block to host range mutant growth was not relieved when agnoprotein was expressed in *trans* (59).

Our present data indicate that the host range mutants are defective in the assembly of viral particles. Whereas in wild-type-infected BSC cells, 75S viral chromatin is converted to 200S-240S viral particles, lesser amounts of this conversion are seen in sucrose gradient fractionations of assembly intermediates from host range mutant-infected cells. Even more striking, no conversion of 75S intermediates is exhibited when host range mutants are grown in nonpermissive CV1 cells. We suggest that the host range activity of T antigen is necessary at the stage of SV40 viral assembly and thus that T antigen also regulates at a much later stage than was previously recognized.

MATERIALS AND METHODS

Cells, viruses, and antisera. BSC40 is an established line of African green monkey kidney cells derived from the BSC1 line (9, 32) and was used for the growth of all virus stocks. CV1C is an independently derived line of African green monkey kidney cells (34).

Wild-type SV40 (strain 776) served as the parent of the host range mutant used in this study. Mutant *dl*1066 carries a small deletion at the carboxy end of the T antigen coding region and has been described previously (12, 51). *pm*1493, an SV40 point mutant in which the agnoprotein initiation codon has been converted from ATG to TTG, was kindly provided by J. Resnick. *pm*1493 was derived from *wt*830 (55).

Rabbit anticapsid serum recognizing SV40 VP1 was generously provided by R. Lanford and J. Butel. A rabbit antiserum recognizing SV40 VP2 and VP3 was kindly provided by H. Kasamatsu (36). T antigen was detected with hamster ascites fluid raised against an SV40-transformed cell line (45).

Growth and titration of virus stocks. Virus stocks were routinely grown by infection of freshly confluent BSC cells in Eagle's minimal essential medium (MEM) plus 10% fetal calf serum in 75-cm^2 flasks with 0.01 to 0.1 PFU of preexisting virus stock per cell. Immediately following infection, the medium was changed to MEM plus 2% fetal calf serum. Around 72 h

postinfection (p.i.), the medium was changed again before the onset of cytopathic morphology. The virus was then allowed to grow about a week longer, until all cells had assumed balloon shapes and had detached from the culture vessel, forming clumps among themselves. The virus-containing medium was freeze-thawed three times to release all virus attached to cellular debris. Titers of pools of freeze-thawed medium were then determined by plaque assay. Stocks for which titers were determined were frozen in aliquots at −20°C.

For determination of titers of virus stocks by plaque assay, BSC40 cells were plated in 6-cm-diameter dishes and infected with appropriate virus dilutions at 80% confluence. After incubation with 1 ml of virus suspension at 37°C for 2 h, the virus-containing medium was removed from the dishes and the cells were fed 3 ml of MEM plus 2% fetal calf serum overnight. On the next day, 12 to 16 h later, the liquid medium was replaced with 3 ml of a 1:1 mixture of 2× Eagle's MEM plus 5% fetal calf serum without phenol red at 37°C or with 1.8% agar at 50°C. The cells were incubated at 37°C and reoverlaid with the agar medium on days 4 and 7 following infection, with the inclusion of 82 μg of neutral red per ml in the final overlay. The purity of the host range stocks was verified by their failure to form plaques on CV1 cells.

Isolation of viral assembly intermediates on sucrose gradients. For separation of viral assembly intermediates on sucrose gradients, BSC or CV1 monkey kidney cells were grown on 10-cm-diameter dishes to near confluence and infected with 1 PFU of mutant or wild-type virus stock per cell in 5 ml of Eagle's MEM plus 2% fetal calf serum per dish. At 40 h p.i., three 10-cm-diameter dishes of each infected cell type were washed twice in Tris-buffered saline (25 mM Tris HCl [pH 7.4], 0.136 M NaCl, 7 mM KCl, 0.7 mM Na_2HPO_4) and lysed in 0.5 ml of hypotonic buffer (25 mM Tris HCl [pH 7.9], 1 mM $MgCl_2$, 0.4 mM $CaCl_2$, 0.5 mM dithiothreitol) per dish at 0°C (21). A total of 1.5 ml of each type of lysate was incubated on ice in a 4°C room while 13-ml 5 to 40% sucrose gradients in 2 mM Tris (pH 7.4) were prepared. The lysates were then scraped into a Dounce homogenizer and processed with 40 strokes. Samples were centrifuged at 2,000 rpm for 5 min in an IEC benchtype centrifuge to pellet nuclei and cell debris. The supernatants were then carefully layered onto the sucrose gradients. The gradients were spun in a Beckman SW40 rotor at 37,000 rpm at 4°C for 70 min. Twenty-five 0.5-ml fractions were hand collected from the bottom of each gradient with the aid of a peristaltic pump.

Western blot (immunoblot) analysis of viral late protein content. One-fifth of each fraction was run on sodium dodecyl sulfate (SDS)–8% polyacrylamide gels alongside prestained molecular weight markers. The gels were electroblotted to nitrocellulose filters (BA85; Schleicher and Schuell) by using a transfer buffer composed of 0.305% Tris base, 1.44% glycine, and 20% methanol. Transfers were done overnight (12 to 16 h) at 8 V and 130 mA.

The filters were probed with rabbit anticapsid serum reactive to VP1 and ^{125}I-protein A by the method of Jagus (32a). Blots were blocked by incubation with shaking in 100 ml of BLOTTO (5% instant nonfat dried milk in 50 mM Tris–200 mM NaCl, pH 7.4) for 3 to 12 h at room temperature and then incubated at room temperature overnight in a seal-a-meal bag with antibody in a minimal volume of BLOTTO. The blots were then rinsed twice for 1 min each time with 50 mM Tris–200 mM NaCl, pH 7.4, and three times for 5 min each time with BLOTTO. They were then incubated for 2 h in 75 ml of BLOTTO plus 250 μl of Triton X-100, 500 μl of 10% SDS, and 200 μl of NEN ^{125}I-protein A (NEX-146L; 2 to 10 μCi/μg) and put through the same rinse protocol with Tris-buffered saline and BLOTTO plus detergents. Finally, the blots were rinsed repeatedly in Tris-buffered saline, dried, mounted, and exposed to Kodak XAR film for autoradiographic visualization of the blotted viral proteins.

Southern blot analysis of viral DNA content. Viral DNA was phenol extracted from four-fifths of each sucrose gradient fraction, precipitated with tRNA carrier, resuspended in TE (10 mM Tris [pH 8.0], 1 mM EDTA), and linearized with *Bam*HI before separation on 0.7% agarose gels. Gels were then capillary blotted to GeneScreen Plus by conventional methods. Probes were prepared by nick translation of 200 ng of plasmid B3, which carried SV40 at the *Bam*HI site of pBR322 (49) in a nick translation mixture including 100 μCi of [α-^{32}P]CTP (NEG-0132; 6,000 Ci/mmol; NEN).

Dried blots were prehybridized for 3 h at 65°C in seal-a-meal bags containing 7 ml of 150 mM $NaPO_4$ (pH 7.2), 725 mM NaCl, 1 mM EDTA, 1% SDS, and 100 μg of heat-denatured salmon sperm DNA per ml and hybridized overnight at 65°C in 7 ml of the same solution plus the boiled SV40 probe. Blots were washed once for 5 min in 200 ml of 2× SSC (1× SSC is 0.15 M NaCl plus 0.015 M sodium citrate) plus 0.1% SDS, twice for 20 min each time in 200 ml of 25 mM $NaPO_4$ (pH 6.5)–1 mM EDTA–0.1% SDS, and twice for 20 min each time in 25 mM $NaPO_4$ (pH 6.5)–1 mM EDTA–1% SDS, all at 65°C. The blots were then exposed to Kodak XAR film while still moist, encased within seal-a-meal bags.

Pulse-chase analysis of the rate of viral assembly. Metabolic labelling of viral DNA with [^{3}H]thymidine was used for pulse-chase analysis of the rate of viral assembly. Infected cells were labelled for 15 min at 40 or 48 h p.i. with 2 ml of 20-μCi/ml [^{3}H]thymidine per dish. At this concentration, incorporation of thymidine was found to be nonlimiting. The labelling medium was then removed, the cells were washed once with 5 ml of phosphate-buffered saline (PBS), and 5 ml of cold-chase MEM plus 2% fetal calf serum was added per dish at 30 min after the initial application of the label. Cells pulse-labelled at 40 h p.i. were chased for 0 and 90 min and 4, 6, 8, and 10 h prior to harvest. Cells labelled at 48 h p.i. were chased for 10, 14, and 18 h prior to harvest.

Labelled infected cell lysates were separated on sucrose gradients as described above. An aliquot was taken from each fraction for scintillation counting in 5 ml of ICN Ecolite fluor.

Immunoprecipitations from sucrose gradient fractions. For immunoprecipitation experiments, infected cells grown on 10-cm-diameter dishes were labelled for 6 h, from 41 to 47 h p.i., with 200 μCi of [^{35}S]methionine (Tran^{35}S-label; ICN) in 2 ml of Dulbecco's MEM minus methionine plus 2% dialyzed fetal calf serum per dish prior to lysis and sucrose gradient fractionation. A total of 1.5 ml of lysate from three dishes was processed and loaded onto each sucrose gradient in the manner described above.

One-fifth of each of the sucrose gradient fractions was immunoprecipitated by our standard protocol. Lysates were preadsorbed and clarified by the addition of 30 μl of Boehringer Mannheim Staph A cells for 30 min and then immunoprecipitated by reaction for 4 to 6 h with 1 μl of the appropriate polyclonal antibody and readdition of 30 μl of Staph A cells for 30 min. Antibodies used were from a hamster ascites fluid recognizing SV40 T antigen and a rabbit anti-SV40 serum recognizing VP1. These amounts of antibody and Staph A cells were previously determined by titration to be nonlimiting. Precipitated pellets were washed twice in 1 ml of SNNTE (5% sucrose, 1% Nonidet P-40, 500 mM NaCl, 50 mM Tris [pH 7.4], 5 mM EDTA) and once in NTE (50 mM NaCl, 10 mM Tris [pH 7.4], 1 mM EDTA) before boiling in SDS loading buffer and separation on SDS–10% polyacrylamide gels. The

gels were treated with the fluor En^{3}Hance (NEN) before drying and exposure to XAR film.

Coimmunoprecipitation of VP1 and viral DNA from sucrose gradient fractions. To compare the VP1 distribution with the viral DNA profiles from the gradients, selected wild-type-infected BSC, *dl*1066-infected BSC, and *dl*1066-infected CV1 sucrose gradient fractions remaining from the [^{3}H]thymidine pulse-chase experiments were immunoprecipitated with anti-SV40 serum recognizing VP1. Samples from a 10-h chase of material labelled at 40 h p.i. were chosen in each case because there was a good distribution of counts between both the assembled and the unassembled peaks. In each case, 50 μl of lysate was preadsorbed and clarified by a preliminary incubation with 30 μl of Staph A cells. Then supernatants were incubated with 1 μl of antibody for 4 h followed by 30 min with 30 μl more of Staph A cells. Supernatants were then pipetted into scintillation vials. This time, immunoprecipitated pellets were washed only once and in a different buffer, composed of 5% sucrose, 1% Nonidet P-40, 150 mM NaCl, 50 mM Tris (pH 7.4), 5 mM $CaCl_2$, and 5 mM $MgCl_2$. Washed pellets were resuspended in 75 μl of 50 mM NaCl–10 mM Tris (pH 7.4)–5 mM $CaCl_2$–5 mM $MgCl_2$ and loaded into scintillation vials for counting.

RESULTS

Previous studies indicated that SV40 host range mutants replicate viral DNA and express viral capsid proteins in nonpermissive cells yet fail to produce infectious virions (38, 50, 61, 64, 65). This suggests that these mutants are blocked in viral assembly or release. To discern the nature of this defect, we examined the accumulation and maturation of viral particles in more detail.

Sucrose gradient analysis reveals that the host range mutants are defective in viral assembly. We first compared the abilities of wild-type SV40 and *dl*1066 to assemble virions in infected BSC and CV1 cells. Cells were infected at a multiplicity of infection of 1 PFU per cell. At 40 h p.i., the cells were lysed in a hypotonic buffer and the viral assembly intermediates were separated on 5 to 40% sucrose gradients. Approximately 25 fractions were collected from each gradient. A portion of each fraction was used for SDS gel electrophoresis and immunodetection of VP1 on Western blots. The remainder was phenol extracted to recover viral DNA which was subsequently visualized by Southern analysis.

Figure 2 displays the distributions of VP1 found on Western blots when infected cell lysates were fractionated on sucrose gradients. In wild-type-infected cells, 56% of the VP1 appeared in the denser fractions 1 to 11, which correspond to fully assembled viral particles (200S-240S). The remainder was distributed among the lighter fractions. BSC cells infected with *dl*1066 showed a similar distribution of VP1. However, somewhat less (42%) of the VP1 appeared in assembled virions. In contrast, *dl*1066-infected CV1 cells contained very little (8%) VP1 in assembled virions.

We also examined the position of viral DNA in these gradients by Southern blot analysis (Fig. 3). In cells infected with wild-type SV40, appreciable amounts of viral DNA appeared in the assembled fractions 6 to 8, with the remainder remaining in the lightest fractions. A similar distribution was found in *dl*1066-infected BSC cells; however, less DNA cosedimented with assembled virions than in wild-type-infected cells. Little or no viral DNA was present in the heaviest fractions from *dl*1066-infected CV1 cells. In the lighter fractions of both *dl*1066-infected BSC and *dl*1066-infected CV1 cells, the viral DNA was found in two peaks. The lightest of these corresponded to the light DNA peak found in wild-type-infected cells. In addition, accumulation of viral DNA in fractions 13 to 18 was evident. We suspect that the absence of SV40 DNA in fraction 16 of the *dl*1066-infected CV1 panel is due to experimental error or the limitations of the technique in light of the results below.

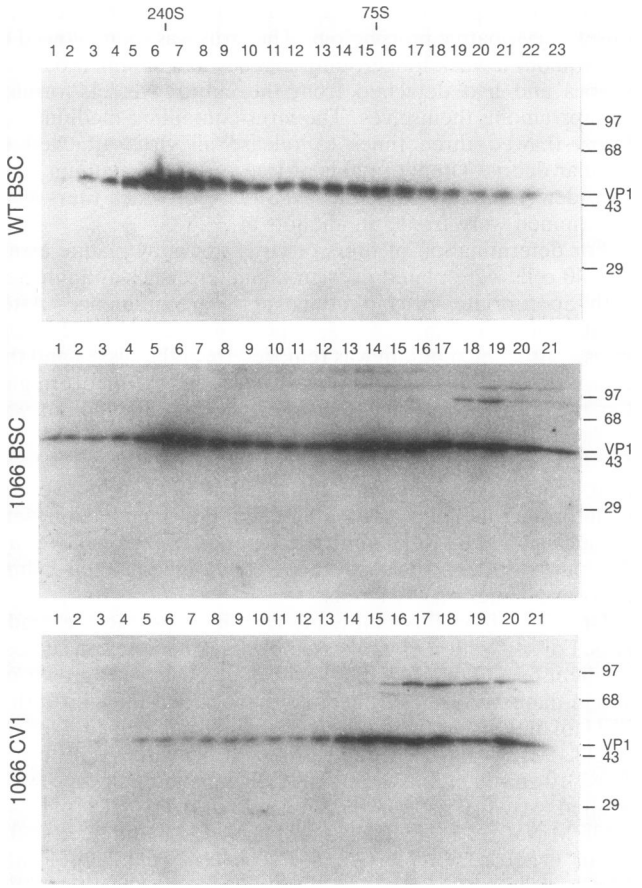

FIG. 2. Western blots of sucrose gradient fractions from wild-type (WT)- and *dl*1066-infected BSC and CV1 cells probed with anti-SV40 antiserum recognizing VP1. Infected cell lysates were separated on 5 to 40% sucrose gradients. Gradient fractions were subjected to SDS–10% polyacrylamide gel electrophoresis, blotted, and probed with anti-SV40 serum. The fractions are numbered from dense to light, with the densest fractions appearing on the left. The high-molecular-weight bands appearing at low density in the *dl*1066-infected BSC and CV1 panels are suspected to represent SDS-resistant dimers and multimers of VP1, which also appear in gradients from wild-type-infected cells on longer exposure or when more lysate is loaded onto the gel. The length of exposure was 24 h.

Pulse-labelling of infected cells prior to sucrose gradient fractionation. We next examined the time course of viral assembly in pulse-chase experiments with wild-type- and *dl*1066-infected BSC and CV1 cells. At 40 h p.i., cells were pulse-labelled with [^{3}H]thymidine for 15 min and chased with MEM plus 2% fetal calf serum for various times. Lysates were prepared and run on 5 to 40% sucrose gradients as described above. The amount of ^{3}H-DNA in each fraction was then assessed. The results are depicted in Fig. 4 to 8.

As shown in Fig. 4, pulse-chase of wild-type SV40 chromatin showed the same conversion of 100S to 75S to 200S-240S forms that was reported by others (4, 21, 23). After a 15-min pulse, mostly 100S material was labelled, which probably represents

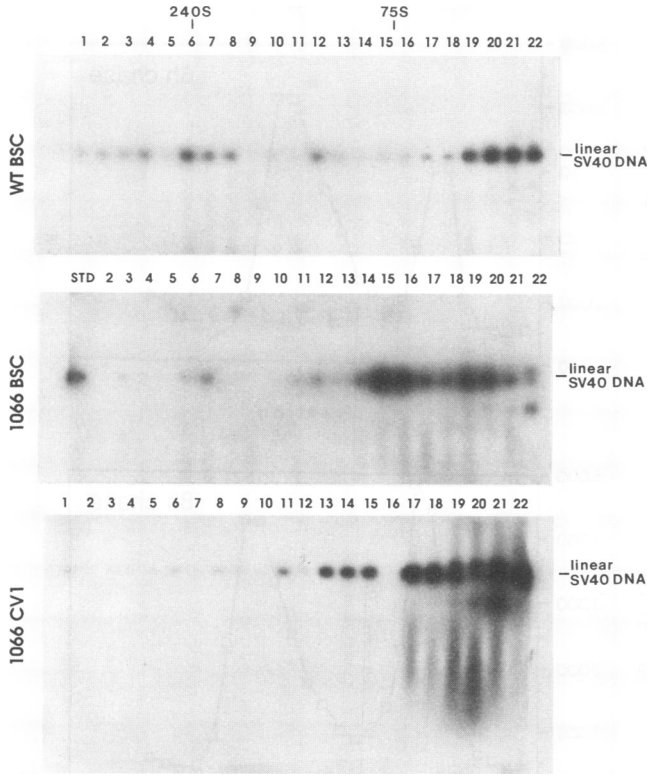

FIG. 3. Southern blots showing SV40 viral DNA in sucrose gradient fractions from wild-type (WT)- and *dl*1066-infected BSC and CV1 cells. Viral DNA was extracted from the gradients shown in Fig. 2, linearized, run on 1% agarose, blotted, and reacted with a radiolabelled SV40 DNA probe.

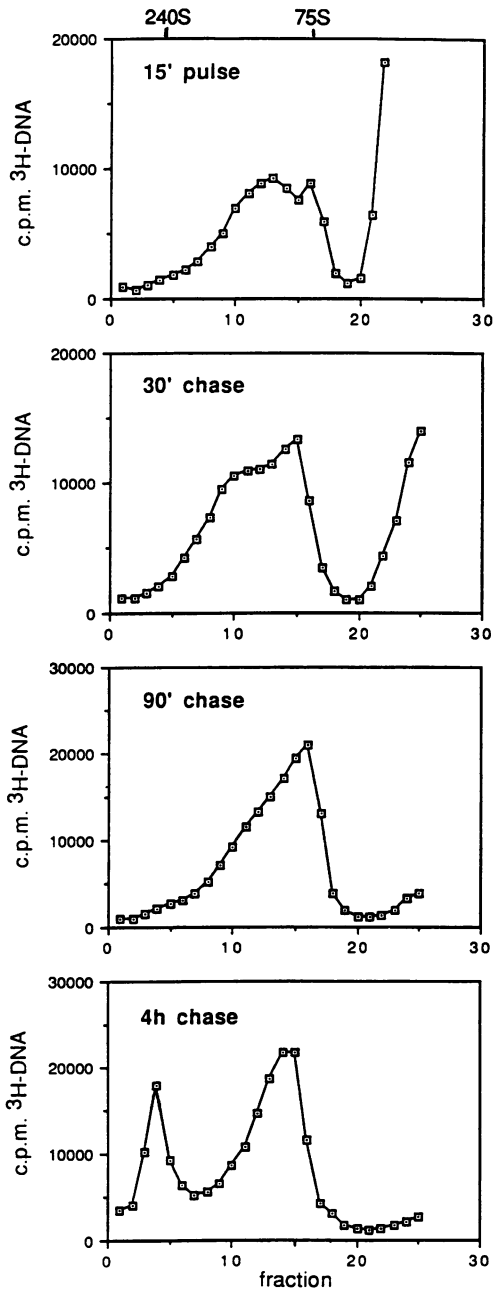

FIG. 4. Pulse-chase experiment showing progression of wild-type virus assembly in BSC cells. Cells were pulse-labelled with [^{3}H]thymidine for 15 min at 40 h p.i. and chased for 0, 30, or 90 min or 4 h. Species labelled are, from top to bottom, 100S, 100S plus 75S, 75S, and 240S plus 75S viral DNAs.

viral chromatin bound to an array of transcription and replication proteins. By 90 min of chase, this material was nearly all converted to 75S viral chromatin, and at 4 h after labelling, a sizeable 200S-240S peak of assembled virus appeared. Others have reported complete conversion of wild-type viral DNA to the 200S-240S peak by 4 h after a 5-min pulse (23). With our longer (15-min) labelling time, however, a larger pool of labelled DNA which takes proportionately longer to convert to the 200S-240S form is accumulated.

In wild-type-infected cells, approximately half of the 75S peak was converted to 200S-240S virions by 7 h after a 15-min pulse (Fig. 5). A similar pattern was observed for CV1 cells infected with wild-type SV40 (Fig. 6). Assembly was much slower in *dl*1066-infected BSC cells (Fig. 7). In CV1 cells, the nonpermissive host for *dl*1066, assembly failed to proceed at al. This resulted in the buildup of 75S viral chromatin over time (Fig. 8). The same pattern as for *dl*1066 was found when assembly was investigated with host range mutant *dl*1140 (data not shown). Similar patterns have previously been reported to be characteristic of *ts*BC11 and *ts*C mutants of SV40, as well as *hr-t* mutants of polyomavirus (6, 23, 26).

To address the possibility that *dl*1066 may not only assemble more slowly than the wild-type virus but may assemble at later times p.i., experiments were repeated using a 15-min pulse at 48 h p.i., rather than at 40 h p.i., and assembly after a 10-, 14-, or 18-h chase was compared with earlier results. Pulse-chase of mutant and wild-type DNAs at these later times p.i. revealed no change in the rate of assembly in any case (data not shown).

Immunoprecipitation of viral proteins from the sucrose gradient fractions. We next sought to examine the protein composition of our wild-type and mutant assembly intermediates by comparing the abilities of viral late proteins to associate with each other under permissive and nonpermissive conditions. In the first experiment, Western blots probed with both an antiserum recognizing VP2 and VP3 and anti-SV40 serum recognizing VP1 were run with concentrated [^{3}H]thymidine-labelled sucrose gradient fractions to directly compare the distribution of these proteins with that of viral DNA in the gradients. Figure 9 shows the results when sucrose gradient

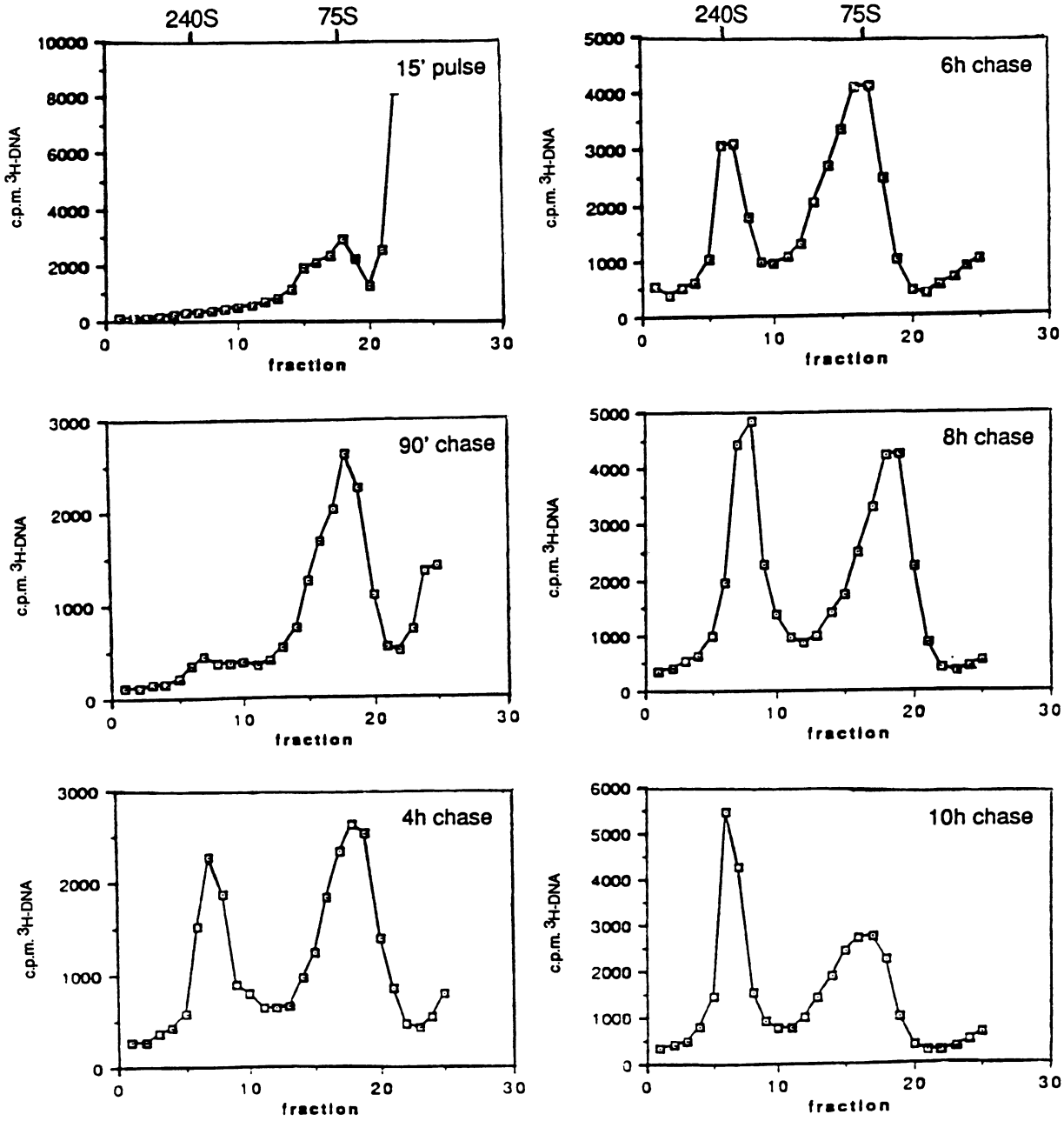

FIG. 5. Pulse-chase of ^{3}H-viral DNA in wild-type-infected BSC cells. Cells were pulse-labelled with [^{3}H]thymidine for 15 min at 40 h p.i. and chased for 0 or 90 min or 4, 6, 8, or 10 h. Counts per minute of ^{3}H are plotted against the fraction number, with the densest fractions appearing on the left.

fractions from wild-type-infected, [^{3}H]thymidine-labelled BSC cells were examined for their VP3 and VP1 contents on a Western blot. A faint VP3 band appeared at about 30 kDa, below the major capsid protein band at 45 kDa. VP3 appeared principally in fractions 4 to 7 and 10 to 19, which correspond to the assembled virion peak and the leading fractions from the unassembled peak of ^{3}H-viral DNA from the same gradient, respectively. VP1 also was found to be most concentrated in assembled virions and the leading fractions from the unassembled DNA peak. In this particular blot, it appeared as a doublet in fractions 16 to 25. This was probably due to the action of a protease which sedimented in the lighter fractions because these fractions were improperly stored prior to electrophoresis. By the protocol employed for this blot, there was enough material to see a minimal VP3 signal in the wild-type gradient shown but not in mutant lysates. VP2 was not visible in either type of lysate under these conditions because it occurs in quantities below the limits of detection. Therefore, we turned to immunoprecipitation experiments for data concerning the distribution of VP2 and VP3 in the gradients of mutant lysates.

When infected cells were labelled with [^{35}S]methionine prior to sucrose gradient fractionation and immunoprecipitation, VP1 was found to be distributed in the expected patterns in

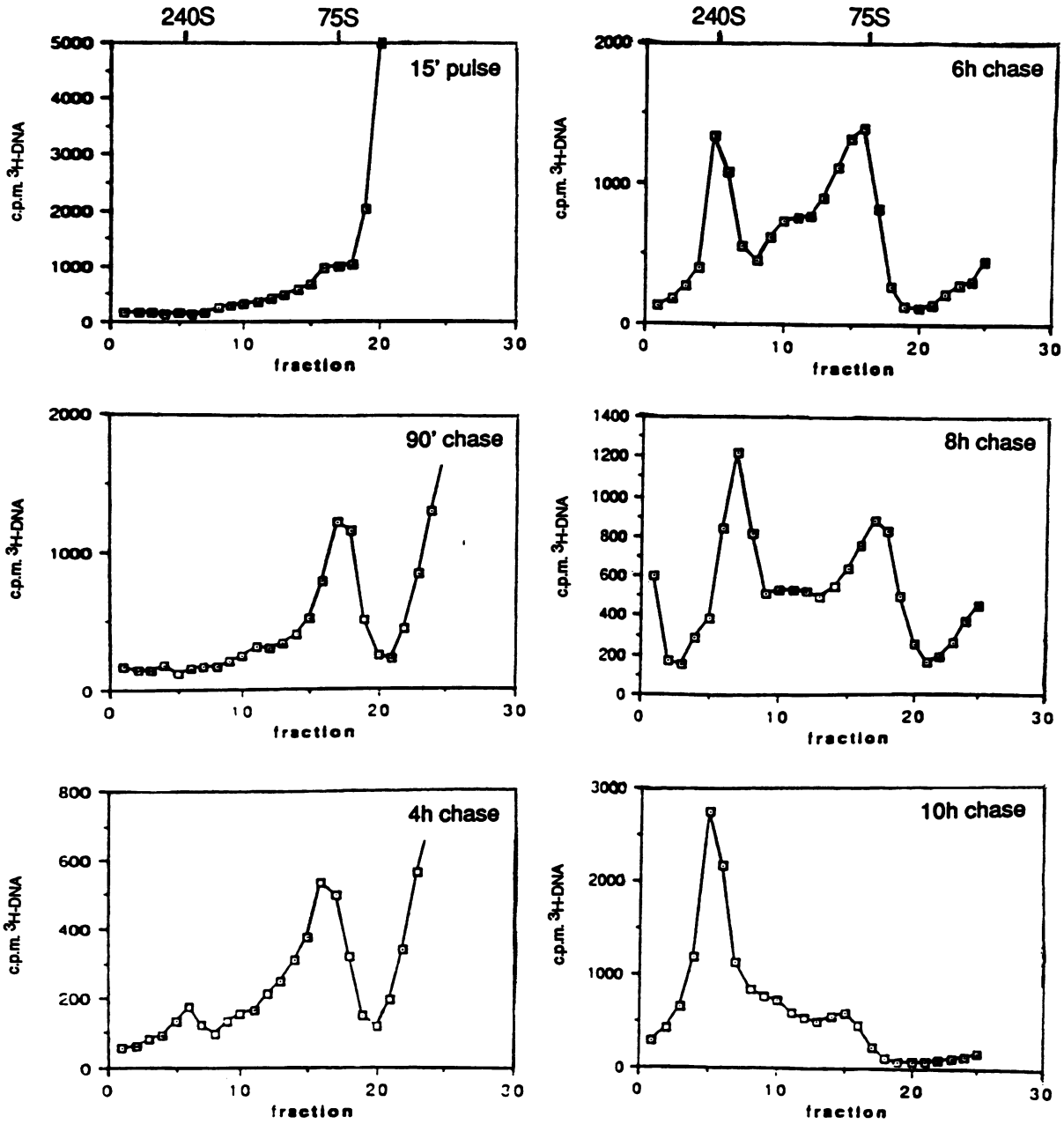

FIG. 6. Pulse-chase of ^{3}H-viral DNA in wild-type-infected CV1 cells. Cells were pulse-labelled with [^{3}H]thymidine for 15 min at 40 h p.i. and chased for 0 or 90 min or 4, 6, 8, or 10 h. Counts per minute of ^{3}H are plotted against the fraction number.

mutant and wild-type gradients. Immunoprecipitations of the odd-numbered fractions from each gradient with anti-SV40 serum recognizing VP1 are shown in Fig. 10. As in previous Western blots, more of the major capsid protein, VP1, appeared in assembled fractions from wild-type-infected CV1 cells than from *dl*1066-infected CV1 cells, in which assembly was impaired. More VP1 appeared in the assembled fractions of wild-type-infected BSC gradients than of *dl*1066-infected BSC gradients, in which partial assembly was expected. Gradients from CV1 cells infected with the virus *pm*1493, which is mutated at the initiation codon for the viral agnoprotein, however, showed no defect in virus assembly.

VP2 and VP3 also appeared in the assembled virus fractions immunoprecipitated with anti-SV40 antibody in all gradients in which assembly occurred. VP2 runs just under the 45-kDa VP1 band, and VP3 runs at about 30 kDa. In these gels, both proteins were most concentrated in the assembled fractions 5 to 9, particularly in the wild-type-infected BSC, wild-type-infected CV1, and *pm*1493-infected CV1 samples, in the case of which the most VP1 was also concentrated there. On darker exposures of the same gels (not shown), VP2 appeared to be present mostly in fractions 3 to 17 and VP3 appeared to be distributed throughout the gradient. A population of contaminating cellular protein bands also appeared in fractions 21 to 25, in which material less dense than viral chromatin assembly intermediates is present. In fractions 15 to 21, a different

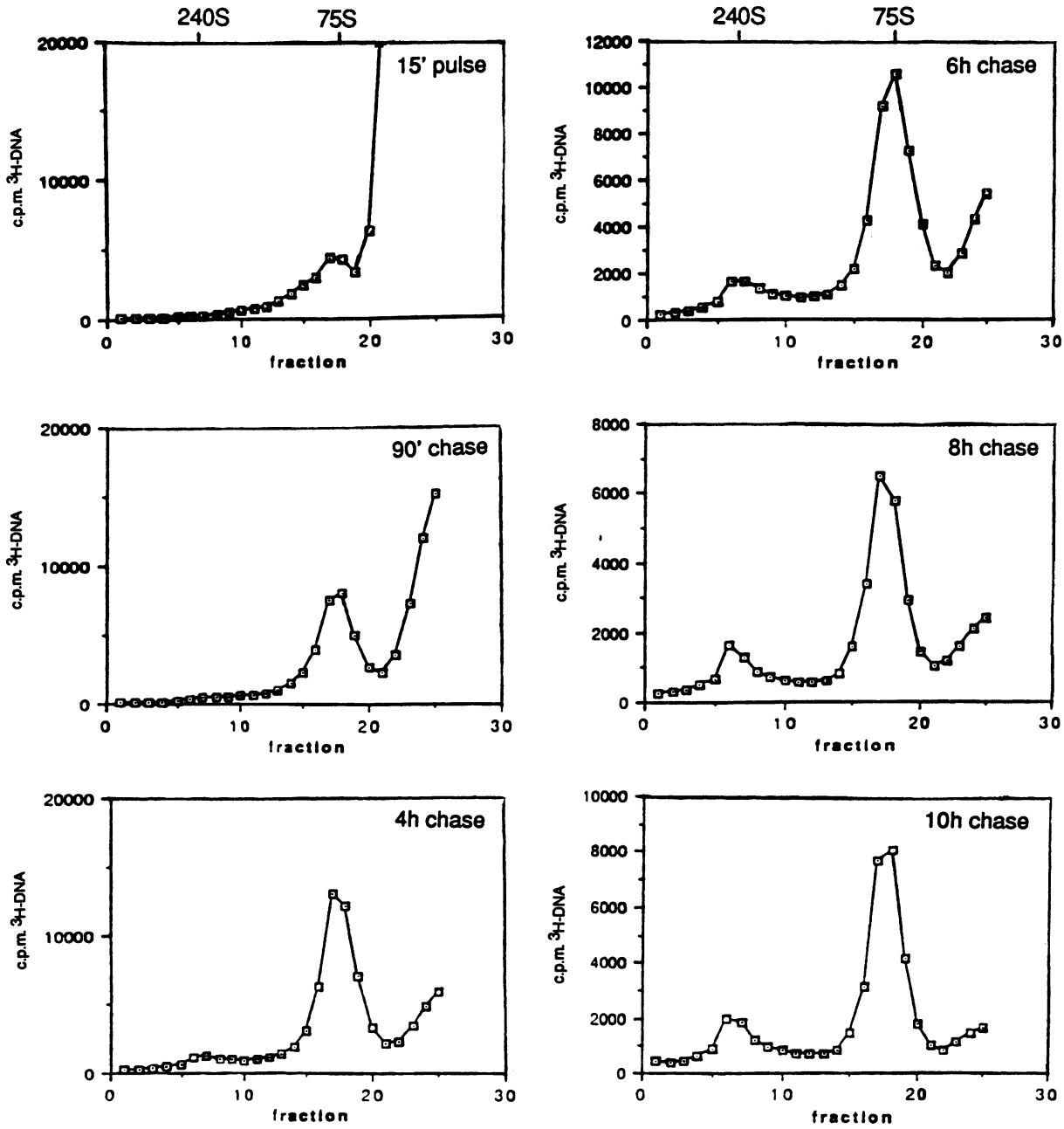

FIG. 7. Pulse-chase of ^{3}H-viral DNA in *dl*1066-infected BSC cells. Cells were pulse-labelled with [^{3}H]thymidine for 15 min at 40 h p.i. and chased for 0 or 90 min or 4, 6, 8, or 10 h. Counts per minute of ^{3}H are plotted against the fraction number.

population of precipitated proteins was found to migrate at approximately 20 to 35 kDa. These cellular bands, probably chromatin associated, coincided with the peak of viral chromatin sedimentation. A strong band, presumably cellular actin, always appeared beneath the immunoprecipitated VP1 band in fractions 19 to 25.

SV40 T antigen and the cellular protein p53 were also seen in the lightest fractions from these immunoprecipitated gradients (Fig. 10). Their identities were confirmed by immunoprecipitation of identical fraction pools with hamster anti-T antigen serum, which precipitated approximately twice as much of both proteins as the anti-SV40 serum (data not shown). The appearance of T antigen in the anti-SV40 precipitates turns out to be the result of a dual specificity in the antiserum which appears in immunoprecipitates (but not on Western blots) rather than evidence of a complex between T antigen and VP1. In lysates from COS cells, which express T antigen in the absence of VP1 (29), this serum precipitated some but not all T antigen present (data not shown).

Coimmunoprecipitation of VP1 and viral DNA from sucrose gradient fractions. When selected [^{3}H]thymidine labelled fractions from a 6-h pulse-chase were immunoprecipitated with anti-SV40 serum recognizing VP1, the results were as shown in Fig. 11. As might be expected, virtually all of the ^{3}H-viral DNA present in the assembled virus peak was precipitated by the anti-SV40 antibody. The 75S unassembled peak was, however,

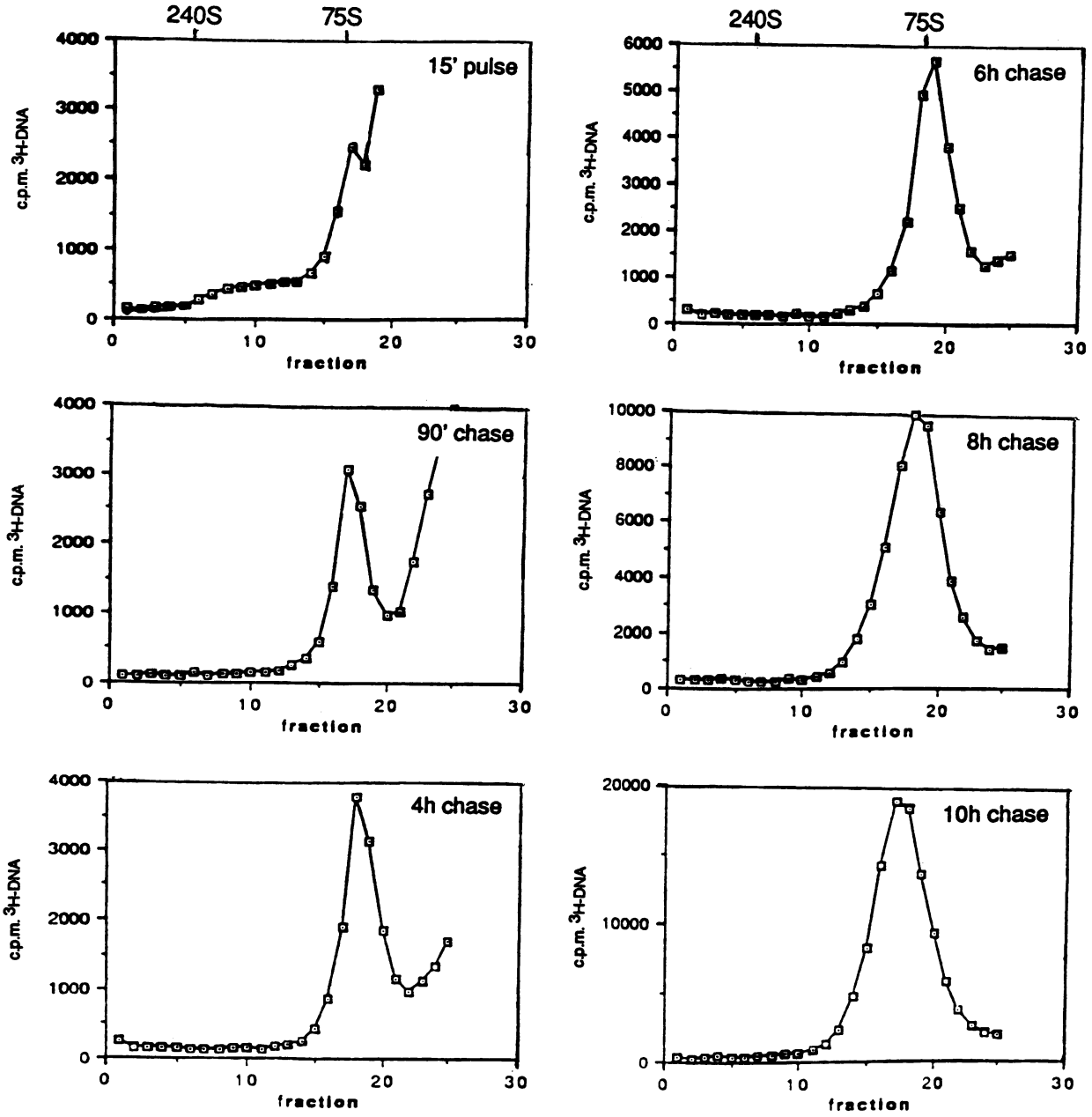

FIG. 8. Pulse-chase of ^{3}H-viral DNA in *dl*1066-infected BSC cells. Cells were pulse-labelled with [^{3}H]thymidine for 15 min at 40 h p.i. and chased for 0 or 90 min or 4, 6, 8, or 10 h. Counts per minute of ^{3}H are plotted against the fraction number.

divided into two classes of viral chromatin, one apparently bound and the other unbound to the major viral capsid protein. The apparently VP1-bound subclass sedimented at a slightly higher density than the unbound chromatin, encompassing the same fractions that were found to contain VP3 in the Western blot in Fig. 9. When *dl*1066-infected BSC and CV1 cell gradient fractions were precipitated with anti-VP1 antibody, however, a much lesser percentage of the 75S chromatin was found to be complexed with VP1 than in wild-type gradient fractions. Whereas in wild-type-infected cells, about 50% of the 75S peak appeared to be VP1 bound, in *dl*1066-infected BSC cells, only about 10% of the 75S material appeared to be bound to VP1. In *dl*1066-infected CV1 cells, VP1 appeared to be bound to less than 5% of the 75S material. This suggests that the host range defect may be attributable to the inability of VP1 to associate with viral chromatin.

DISCUSSION

Prior to this work, T antigen's role in productive infection was thought to be limited to DNA replication and transcriptional control. We and others, however, have reported mutants of T antigen which exhibit defects in viral plaque formation at stages later than viral replication (18, 50, 64). Here we have further characterized the C-terminal host range mutants and have determined that T antigen encodes an additional activity

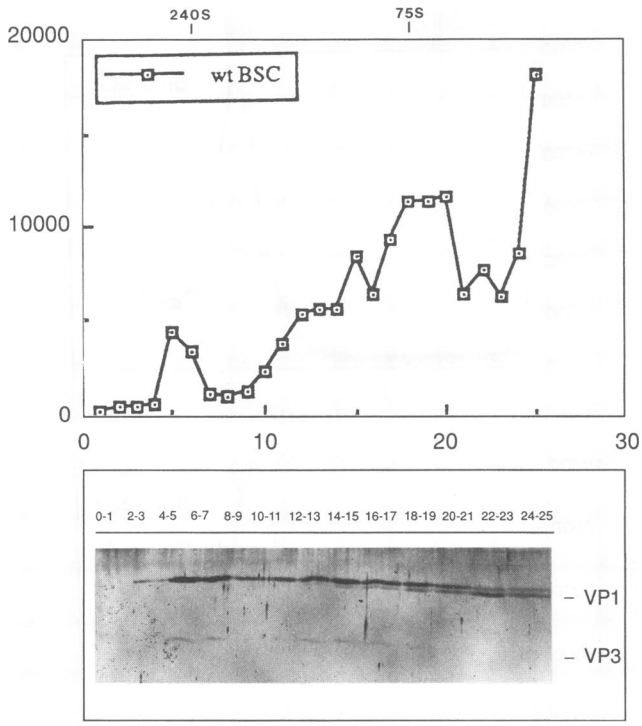

FIG. 9. Locations of VP1 and VP3 among gradient fractions from wild-type (WT)-infected cells. Sucrose gradient fractions from wild-type-infected cells continuously labelled with [^{3}H]thymidine were concentrated and run on an SDS–10% gel. The gel was blotted and probed with an antibody recognizing VP2 and VP3 followed by ^{125}I-protein A. Later the same blot was reprobed with anti-SV40 antibody recognizing VP1, which was visualized by a peroxidase-conjugated second antibody and a color reaction. VP1 and VP3 are indicated. VP2 occurs in trace amounts and is not visible here. The blot is aligned with the ^{3}H-viral DNA profile taken from the same gradient (top panel).

which is necessary for the assembly of SV40 viral particles. In addition, our data help to clarify the mechanism whereby wild-type SV40 virions are assembled. Last, we offer some suggestions as to the stage at which host range mutant assembly is blocked.

SV40 is assembled as a 45-nm, 240S, 1.33-g/cm^3 icosahedral particle containing one histone-bound copy of supercoiled, double-stranded DNA and the viral capsid proteins VP1, VP2, and VP3 in an approximately 24:1:4 ratio (8, 63). X-ray crystallographic studies have determined that both the capsid of SV40 (46) and that of polyomavirus (54) are composed of 360 molecules of VP1 arranged in 72 surface pentamers held in 12 pentavalent and 60 hexavalent positions by the three alternative bonding patterns of which VP1 is capable. Although the locations of VP2 and VP3 are not clearly apparent from the crystal structure, there are patterns of electron density beneath each pentamer which suggest that they occur at more internal positions in the virion (3, 46).

Over the years, a variety of models have been proposed for in vivo SV40 and polyomavirus assembly (reviewed in reference 8). As determined from observations of viral assembly intermediates on sucrose gradients after pulse-chase of [^{3}H]thymidine, 100S replicating chromatin is converted to a 75S chromatin assembly intermediate which is then converted to 200S previrions and a 240S assembled virion species (4, 13, 19, 21, 23, 24, 33). The same program for viral assembly was also reported for polyomavirus, in which pulse-chase showed the conversion of 90S assembly intermediates to 200S and 240S forms (26, 66). The 75S particle is not infectious, whereas 200S-240S particles are (4, 42). The 200S and 240S species usually comigrated; however, a distinct 200S species could sometimes be discerned at early times over the course of pulse-chase (21, 23), and this species appeared to be sensitive to high salt concentrations and unstable when recentrifuged in CsCl gradients (4, 19, 33, 43, 57).

Some confusion has centered over the specific order and stages in which capsid proteins are added to assembly intermediates. Over the course of virion assembly, histones H2A, H2B, H3, and H4 become more highly acetylated, apparently by protection from deacetylase activity, and histone H1 is displaced or degraded, such that it appears in 75S and 200S particles but not in virions (13, 14, 21, 42, 43). This proceeds concurrently with the progressive addition of VP1, VP2, and VP3 to the 75S viral minichromosome. In spite of their own data and those of Fernandez-Munoz and coworkers (21) indicating the association of some VP1 with 75S assembly intermediates, Garber et al. (24) originally concluded that the 75S peak was essentially histone-bound viral chromatin. From the sequential appearance of capsid proteins in 200S-240S gradient fractions after pulse-chase with [^{3}H]leucine, they concluded that 75S intermediates became 200S previrions by the addition of VP1 and VP3 and then 240S virions by the further addition of all three capsid proteins. On the basis of Western blot analysis of the capsid protein content of 90S, 200S, and 240S material, Yuen and Consigli (66) concluded, on the other hand, that the 90S polyomavirus intermediate was bound to some VP1 and to its full quotient of VP2 and VP3. According to their data, conversion to the 200S and 240S forms involved addition and subtraction of additional isoelectric species of VP1.

Our data help to distinguish between the Garber and the Yuen and Consigli models and present a new instance in which SV40 viral assembly is blocked. We find that in sucrose gradient fractions from wild-type-infected cells, the leading shoulder of the 75S viral assembly peak contains both VP3 and VP1, which is what one would expect if SV40 assembly were to follow the program proposed for polyomavirus assembly (27, 66). Moreover, our data clearly indicate that only the denser shoulder of the 75S peak is associated with VP1, VP3, (perhaps, VP2) and DNA, indicating that the 75S material really represents at least two different populations of intermediates in the assembly pathway.

For some time, two groups of T-antigen mutants with postreplicative defects have been known, namely, the mutant *ts*A1642 and the SV40 host range/adenovirus helper function mutants. The temperature-sensitive mutation *ts*A1642 (18) maps to a conserved proline in the middle of T antigen (Pro-453 to Ser). Unlike most temperature-sensitive mutants of T antigen, *ts*A1642 was reported to replicate at 30% of wild-type levels, to make a stable T antigen and to make substantial amounts of viral late proteins at the nonpermissive temperature (41°C) in TC7 cells (18). Synthesis of VP1, VP2, and VP3 appeared to be reduced only 5- to 10-fold relative to that of the wild type, yet a 3-log decrease in virus yield was observed upon growth of the virus at the nonpermissive temperature. The mutant virus was unable to transform mouse embryo fibroblasts, but *ts*A1642 was not defective in adenovirus helper function.

The host range mutants, which map to the C terminus of T antigen (16, 17, 50, 51, 64), produce stable, truncated T antigens and replicate to near wild-type levels (12, 50). However, they are cold sensitive for growth on BSC monkey kidney

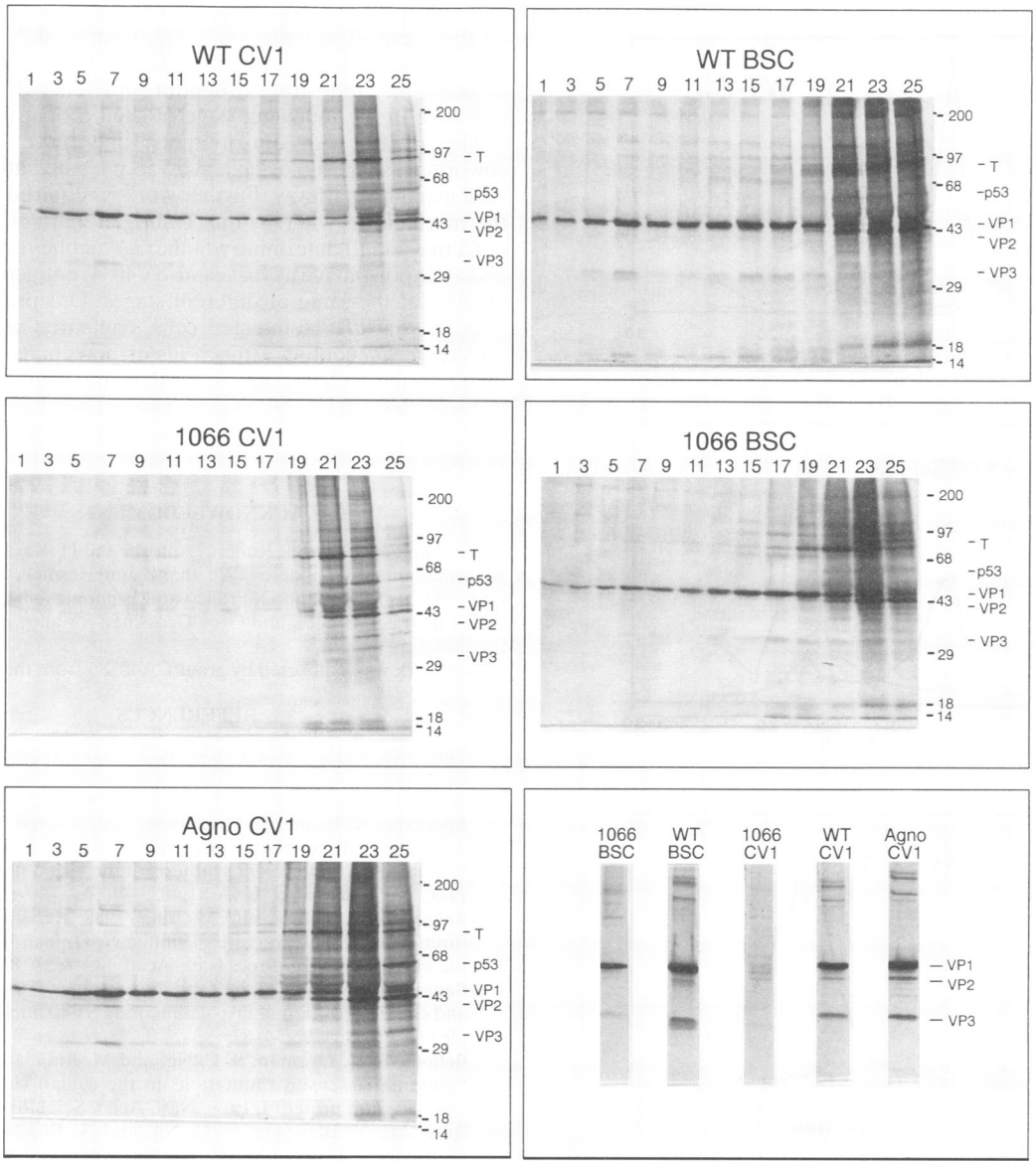

FIG. 10. Immunoprecipitation of ^{35}S-labelled viral proteins from *dl*1066-infected BSC, wild-type (WT)-infected BSC, *dl*1066-infected CV1, wild-type-infected CV1, and *pm*1493-infected CV1 sucrose gradient fractions. Infected cells were labelled with [^{35}S]methionine prior to sucrose gradient fractionation. In these SDS gels, every other gradient fraction was precipitated with anti-SV40 antibody recognizing VP1 and T antigen. In the bottom right panel, a darker exposure of the lane corresponding to fraction 7 from the same gradients is shown. The panel depicting the gradient from *pm*1493-infected CV1 cells is labelled Agno CV1, reflecting that this virus is mutated in the initiation codon for the viral agnoprotein.

cells (50, 62) and, unlike wild-type virus, are unable to grow on CV1 monkey kidney cells at any temperature (50, 64). Levels of late transcripts and late protein accumulation are decreased 5- to 10-fold in host range mutant-infected nonpermissive CV1 cells (38, 61, 65). The late leader agnoprotein is undetectable in these cells (38, 61); however, growth of the host range mutants and manufacture of normal levels of capsid protein are not complemented in agnoprotein-transformed CV1 cells (59, 62). None of the host range mutants are transformation defective. However, all which have been tested are defective in adenovirus helper activity.

Here we show that the host range mutants are blocked in the assembly of SV40 viral particles. SV40 virions are assembled inefficiently in host range mutant-infected (permissive) BSC cells. They appear not to be assembled at all in host range mutant-infected (nonpermissive) CV1 cells. In pulse-chase experiments to monitor virion assembly, wild-type SV40 chromatin follows the established pattern of progression from 100S to 75S to 200S-240S assembled virion material. In pulse-chase experiments, the host range mutants *dl*1066 and *dl*1140, on the other hand, build up large amounts of 75S chromatin, without conversion to the 200S-240S form, particularly in nonpermissive cells. This heavy accumulation of viral chromatin in the nuclei of the host range mutants, without the ability to be assembled and released, may explain the early cytopathic effect which is so often seen in these cultures (16, 50).

The accumulation of 75S assembly intermediates by host range mutants is reminiscent of similar patterns which have

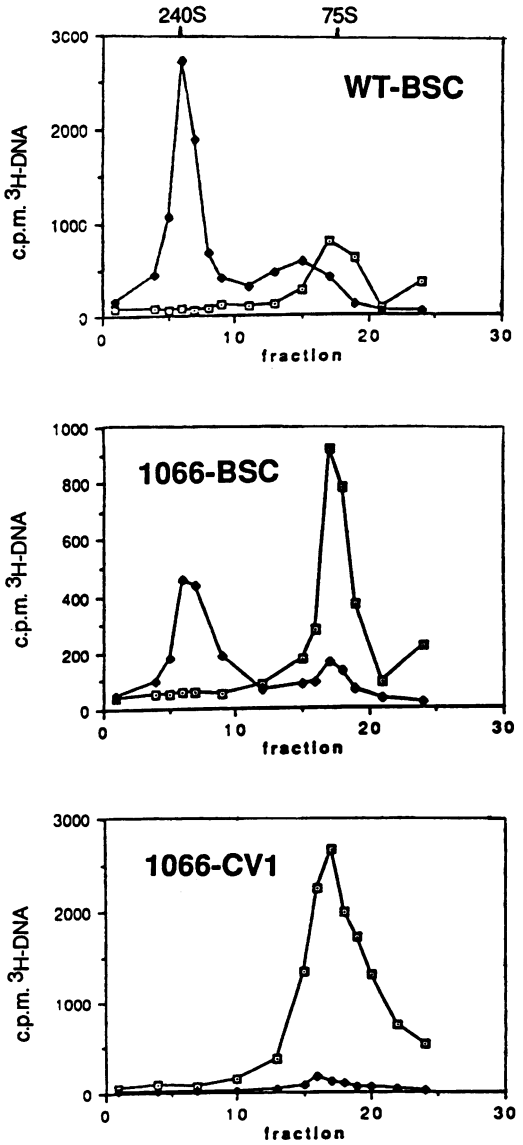

FIG. 11. Coimmunoprecipitations of *dl*1066 and wild-type (WT) viral DNAs with VP1. ^{3}H-viral DNAs were immunoprecipitated by anti-SV40 serum recognizing VP1 from wild-type-infected BSC, *dl*1066-infected BSC, and *dl*1066-infected CV1 sucrose gradient fractions. Counts per minute of ^{3}H are plotted against the fraction number. The solid diamonds indicate counts per minute per fraction of ^{3}H-DNA in the precipitated pellets. The open squares indicate counts per minute of DNA still left in the supernatant.

been reported to be characteristic of *ts*BC11 and *ts*C mutants of SV40, as well as of the *hr-t* mutants of polyomavirus. Bina and coworkers have shown that *ts*B, *ts*C, and *ts*BC mutants are assembly defective because of temperature-sensitive lesions in the SV40 VP1 capsid gene (5, 11, 44). Upon [^{3}H]thymidine labelling at the nonpermissive temperature, *ts*BC11 and the *ts*C mutants accumulate 75S viral chromatin bound to few, if any, capsid proteins, which fails to convert to 200S-240S virions (6, 23, 48). This is similar to the pattern which has been reported for the *hr-t* mutants of polyomavirus, which carry mutations in the gene encoding middle T antigen and are said to lack proper VP1 phosphorylation (25, 26, 28). On the other hand, all *ts*B and most *ts*BC mutants appear to accumulate both 75S particles and a novel 100S-160S assembly intermediate containing all three capsid proteins (6, 7, 48). Bina et al. have suggested that the *ts*C mutants are defective in the initiation of shell assembly around viral chromatin and that *ts*B mutants are defective in the following stage of shell propagation.

The results with our mutants, like those of Bina and coworkers, suggest blockage at a 75S intermediate in the SV40 viral assembly pathway. Further work is required to determine the mechanisms whereby our T antigen mutants are assembly defective and to determine whether assemblies of the SV40 *ts*B and *ts*C, polyomavirus *hr-t*, and SV40 T antigen mutants are blocked at the same or different stages. Our preliminary data indicate that *dl*1066-infected cells, compared with wild-type-infected cells, contain a much lesser percentage of 75S chromatin bound to VP1, suggesting that the host range mutation prevents VP1 from binding to nascent viral chromatin. The host range domain may act directly on assembly or by influencing a cellular activity which exerts an indirect effect.

ACKNOWLEDGMENTS

We thank Janet Butel, Robert Lanford, and H. Kasamatsu for their generous gift of antibodies. We thank Jim Resnick for the *pm*1493 virus. We also thank the DeFranco and Edmonds laboratories for the use of their centrifuges, and Greg Grossman for allowing us to use his fractionation system.

This work was supported by grant CA40586 from the NIH to J.M.P.

REFERENCES

1. **Anderson, K. P., and D. F. Klessig.** 1983. Posttranscriptional block to synthesis of a human adenovirus capsid protein in abortively infected monkey cells. J. Mol. Appl. Genet. **2**:31–42.
2. **Anderson, K. P., and D. F. Klessig.** 1984. Altered mRNA splicing in monkey cells abortively infected with human adenovirus may be responsible for inefficient synthesis of the virion fiber polypeptide. Proc. Natl. Acad. Sci. USA **81**:4023–4027.
3. **Baker, T. S., J. Drak, and M. Bina.** 1988. Reconstruction of the three dimensional structure of simian virus 40 and visualization of the chromatin core. Proc. Natl. Acad. Sci. USA **85**:422–426.
4. **Baumgartner, I., C. Kuhn, and E. Fanning.** 1979. Identification and characterization of fast-sedimenting SV40 nucleoprotein complexes. Virology **96**:54–63.
5. **Behm, M., H. Lowman, S. C. Ng, and M. Bina.** 1988. Analysis of temperature-sensitive mutations in the simian virus 40 gene encoding virion protein I. Proc. Natl. Acad. Sci. USA **85**:9421–9425.
6. **Bina, M., V. Blasquez, S. C. Ng, and S. Beecher.** 1982. SV40 morphogenesis. Cold Spring Harbor Symp. Quant. Biol. **47**:565–569.
7. **Blasquez, V., S. Beecher, and M. Bina.** 1983. Simian virus 40 morphogenetic pathway: an analysis of assembly-defective tsB201 DNA-protein complexes. J. Biol. Chem. **258**:8477–8484.
8. **Brady, J. N., and N. P. Salzman.** 1986. The papovaviruses: general properties of polyoma and SV40, p. 1–26. *In* N. P. Salzman (ed.), The Papovaviridae. Plenum Press, New York.
9. **Brockman, W. W., and D. Nathans.** 1974. The isolation of simian virus 40 variants with specifically altered genomes. Proc. Natl. Acad. Sci. USA **71**:942–946.
10. **Brough, D. F., S. A. Rice, S. Sell, and D. F. Klessig.** 1985. Restricted changes in the adenovirus DNA-binding protein that lead to extended host range or temperature-sensitive phenotypes. J. Virol. **55**:206–212.
11. **Chou, J. Y., and R. G. Martin.** 1975. Products of complementation between temperature-sensitive mutants of simian virus 40. J. Virol. **15**:127–136.
12. **Clark, R., K. Peden, J. M. Pipas, D. Nathans, and R. Tjian.** 1983. Biochemical activities of T-antigen proteins encoded by simian virus 40 A gene deletion mutants. Mol. Cell. Biol. **3**:220–228.
13. **Coca-Prados, M., and M. T. Hsu.** 1979. Intracellular forms of simian virus 40 nucleoprotein complexes. II. Biochemical and electron microscopic analysis of simian virus 40 virion assembly. J. Virol. **31**:199–208.

14. **Coca-Prados, M., G. Vidali, and M. T. Hsu.** 1980. Intracellular forms of simian virus 40 nucleoprotein complexes. III. Study of histone modifications. J. Virol. **36**:353–360.
15. **Cole, C. N., L. V. Crawford, and P. Berg.** 1979. Simian virus 40 mutants with deletions at the 3′ end of the early region are defective in adenovirus helper function. J. Virol. **30**:683–691.
16. **Cole, C. N., and T. P. Stacy.** 1987. Biological properties of simian virus 40 host range mutants lacking the COOH-terminus of large T antigen. Virology **161**:170–180.
17. **Cole, C. N., J. Tornow, R. Clark, and R. Tjian.** 1986. Properties of the simian virus 40 (SV40) large T antigens encoded by SV40 mutants with deletions in gene A. J. Virol. **57**:539–546.
18. **Cosman, D. J., and M. J. Tevethia.** 1981. Characterization of a temperature-sensitive DNA-positive nontransforming mutant of simian virus 40. Virology **112**:605–624.
19. **Fanning, E., and I. Baumgartner.** 1980. Role of fast-sedimenting SV40 nucleoprotein complexes in virus assembly. Virology **102**:1–12.
20. **Fanning, E., and R. Knippers.** 1992. Structure and function of simian virus 40 large tumor antigen. Annu. Rev. Biochem. **61**:55–85.
21. **Fernandez-Munoz, R., M. Coca-Prados, and M. T. Hsu.** 1979. Intracellular forms of simian virus 40 nucleoprotein complexes. I. Methods of isolation and characterization in CV-1 cells. J. Virol. **29**:612–623.
22. **Fried, M., and C. Prives.** 1986. The biology of simian virus 40 and polyomavirus. Cancer Cells **6**:1–16.
23. **Garber, E. A., M. M. Seidman, and A. J. Levine.** 1978. The detection and characterization of multiple forms of SV40 nucleoprotein complexes. Virology **90**:305–316.
24. **Garber, E. A., M. M. Seidman, and A. J. Levine.** 1980. Intracellular SV40 nucleoprotein complexes: synthesis to encapsidation. Virology **107**:389–401.
25. **Garcea, R. L., K. Ballmer-Hofer, and T. L. Benjamin.** 1985. Virion assembly defect of polyomavirus *hr-t* mutants: underphosphorylation of major capsid protein VP_1 before viral DNA encapsidation. J. Virol. **54**:311–316.
26. **Garcea, R. L., and T. L. Benjamin.** 1983. Host range transforming gene of polyoma plays a role in virus assembly. Proc. Natl. Acad. Sci. USA **80**:3613–3617.
27. **Garcea, R. L., and T. L. Benjamin.** 1983. Isolation and characterization of polyoma nucleoprotein complexes. Virology **130**:65–75.
28. **Garcea, R. L., D. A. Talmadge, A. Harmoto, R. Freund, and T. L. Benjamin.** 1989. Separation of host range from transformation functions of the hr-t gene of polyoma virus. Virology **168**:312–319.
29. **Gluzman, Y.** 1981. SV40-transformed simian cells support the replication of early SV40 mutants. Cell **23**:175–182.
30. **Grodzicker, T., C. Anderson, P. A. Sharp, and J. Sambrook.** 1974. Conditional lethal mutants of adenovirus 2-simian virus 40 hybrids. I. Host range mutants of Ad2$^+$ND1. J. Virol. **13**:1237–1244.
31. **Heath, C. V., E. Fanning, and C. N. Cole.** 1992. Adenovirus helper function of simian virus 40 T antigen mutants. Virology **189**:762–765.
32. **Hopps, H. E., B. C. Bernheim, A. Nisalak, J. H. Tjio, and J. E. Smadel.** 1963. Biological characteristics of a continuous kidney cell line derived from the African green monkey. J. Immunol. **91**:416–424.
32a. **Jagus, R.** Unpublished data.
33. **Jakobovits, E. B., and Y. Aloni.** 1980. Isolation and characterization of various forms of simian virus 40 DNA-protein complexes. Virology **102**:107–118.
34. **Jensen, F. C., A. J. Girardi, R. V. Gilden, and H. Koprowski.** 1964. Infection of human and simian tissue cultures with Rous sarcoma virus. Proc. Natl. Acad. Sci. USA **52**:53–59.
35. **Johnston, J. M., K. P. Anderson, and D. F. Klessig.** 1985. Partial block to transcription of human adenovirus type 2 late genes in abortively infected monkey cells. J. Virol. **56**:378–385.
36. **Kasamatsu, H., and A. Nehorayan.** 1979. Intracellular localization of viral polypeptides during simian virus 40 infection. J. Virol. **32**:648–660.
37. **Kelly, T. R., Jr., and A. M. Lewis, Jr.** 1973. Use of nondefective adenovirus-simian virus 40 hybrids for mapping the simian virus 40 genome. J. Virol. **12**:643–652.
38. **Khalili, K., J. Brady, J. M. Pipas, S. L. Spence, M. Sadofsky, and G. Khoury.** 1988. Carboxyl-terminal mutants of the large tumor antigen of simian virus 40: a role for the early protein late in the lytic cycle. Proc. Natl. Acad. Sci. USA **85**:354–358.
39. **Klessig, D. F., and C. W. Anderson.** 1975. Block to multiplication of adenovirus serotypes in monkey cells. J. Virol. **16**:1650–1688.
40. **Klessig, D. F., and L. T. Chow.** 1980. Incomplete splicing and deficient accumulation of fiber messenger RNA in monkey cells infected by human adenovirus type 2. J. Mol. Biol. **139**:221–242.
41. **Klessig, D. F., and T. Grodzicker.** 1979. Mutations that allow human Ad2 and Ad5 to express late genes in monkey cells map to the viral gene encoding the 72K DNA binding protein. Cell **17**:957–966.
42. **La Bella, F., and C. Vesco.** 1980. Late modifications of simian virus 40 chromatin during the lytic cycle occur in an immature form of virion. J. Virol. **33**:1138–1150.
43. **La Bella, F., G. Vidali, and C. Vesco.** 1979. Histone acetylation in CV1 cells infected with simian virus 40. Virology **96**:565–575.
44. **Lai, C. J., and D. Nathans.** 1976. The B/C gene of simian virus 40. Virology **75**:335–345.
45. **Lanford, R. E., and J. S. Butel.** 1979. Antigenic relationship of SV40 early proteins to purified large T polypeptide. Virology **97**:295–306.
46. **Liddington, R. C., Y. Yan, J. Moulas, R. Sahli, T. L. Benjamin, and S. C. Harrison.** 1991. Structure of simian virus 40 at 3.8 Å resolution. Nature (London) **354**:278–284.
47. **Manos, M. M., and Y. Gluzman.** 1985. Genetic and biochemical analysis of transformation-competent, replication-defective simian virus 40 large T antigen mutants. J. Virol. **53**:120–127.
48. **Ng, S.-C., and M. Bina.** 1984. Temperature-sensitive BC mutants of simian virus 40: block in virion assembly and accumulation of capsid-chromatin complexes. J. Virol. **50**:471–477.
49. **Peden, K. W. C., J. M. Pipas, S. Pearson-White, and D. Nathans.** 1980. Isolation of mutants of an animal virus in bacteria. Science **209**:1392–1396.
50. **Pipas, J. M.** 1985. Mutations near the carboxyl terminus of the simian virus 40 large tumor antigen alter viral host range. J. Virol. **54**:569–575.
51. **Pipas, J. M., K. W. Peden, and D. Nathans.** 1983. Mutational analysis of simian virus 40 T antigen: isolation and characterization of mutants with deletions in the T-antigen gene. Mol. Cell. Biol. **3**:203–213.
52. **Polvino-Bodnar, M., and C. N. Cole.** 1982. Construction and characterization of viable deletion mutants of simian virus 40 lacking sequences near the 3′ end of the early region. J. Virol. **62**:489–502.
53. **Rabson, A. S., G. T. O'Connor, I. K. Berezesky, and F. J. Paul.** 1964. Enhancement of adenovirus growth in African green monkey kidney cell cultures by SV40. Proc. Soc. Exp. Biol. Med. **116**:187–190.
54. **Rayment, I., T. S. Baker, D. L. Caspar, and W. T. Murakami.** 1982. Polyoma virus capsid structure at 22.5 Å resolution. Nature (London) **295**:110–115.
55. **Resnick, J., and T. Shenk.** 1986. Simian virus 40 agnoprotein facilitates normal nuclear location of the major capsid polypeptide and cell-to-cell spread of virus. J. Virol. **60**:1098–1106.
56. **Schneider, J., and E. Fanning.** 1988. Mutations in the phosphorylation sites of simian virus 40 (SV40) T antigen alter its origin DNA-binding specificity for site I or II and affect SV40 DNA replication activity. J. Virol. **62**:1598–1605.
57. **Seidman, M., E. Garber, and A. J. Levine.** 1979. Parameters affecting stability of SV40 virions during the extraction of nucleoprotein complexes. Virology **95**:256–259.
58. **Silverman, L., and D. F. Klessig.** 1989. Characterization of the translational defect to fiber synthesis in monkey cells infected with human adenovirus: role of ancillary leaders. J. Virol. **63**:4376–4385.
59. **Spence, S. L., L. C. Tack, J. H. Wright, S. Carswell, and J. M. Pipas.** 1990. Infection of CV1 cells expressing the polyoma virus middle T antigen or the SV40 agnogene product with simian virus 40 host-range mutants. In Vitro **26**:604–611.
60. **Srinivasan, A., K. W. Peden, and J. M. Pipas.** 1989. The large tumor antigen of simian virus 40 encodes at least two distinct

transforming functions. J. Virol. **63:**5459–5463.
61. **Stacy, T., M. Chamberlain, and C. N. Cole.** 1989. Simian virus 40 host range/helper function mutants cause multiple defects in viral late gene expression. J. Virol. **63:**5208–5215.
62. **Stacy, T. P., M. Chamberlain, S. Carswell, and C. N. Cole.** 1990. The growth of simian virus 40 (SV40) host range/adenovirus helper function mutants in an African green monkey cell line that constitutively expresses the SV40 agnoprotein. J. Virol. **64:**3522–3526.
63. **Tooze, J.** 1981. DNA tumor viruses: molecular biology of tumor viruses. Cold Spring Harbor Laboratory, Cold Spring Harbor, N.Y.
64. **Tornow, J., and C. N. Cole.** 1983. Nonviable mutants of simian virus 40 with deletions near the 3′ end of gene A define a function for large T antigen required after onset of viral DNA replication. J. Virol. **30:**936–941.
65. **Tornow, J., M. Polvino-Bodnar, G. Santangelo, and C. N. Cole.** 1985. Two separable functional domains of simian virus 40 large T antigen: carboxyl-terminal region of simian virus 40 large T antigen is required for efficient capsid protein synthesis. J. Virol. **53:**415–424.
66. **Yuen, L. K. C., and R. A. Consigli.** 1985. Identification and protein analysis of polyomavirus assembly intermediates from infected primary mouse embryo cells. Virology **144:**127–136.
67. **Zhu, J., P. W. Rice, L. Gorsch, M. Abate, and C. N. Cole.** 1992. Transformation of a continuous rat embryo fibroblast cell line requires three separate domains of simian virus 40 large T antigen. J. Virol. **66:**2780–2791.